Tree-ring $\delta^{18}O$ reveals no long-term change of atmospheric water demand since 1800 in the northern Great Hinggan Mountains, China

Xiaohong LIU [1, 2*], Xuanwen ZHANG [2, 3], Liangju ZHAO [4], Guobao XU [2], Lixin WANG [5], Weizhen SUN [2], Qiuliang ZHANG [6], Wenzhi WANG [7], Xiaomin ZENG [2, 3], Guoju WU [2, 3]

1. Department of Geography, Shaanxi Normal University, Xi'an 710119, China

2. State Key Laboratory of Cryospheric Sciences, Northwest Institute of Eco-Environment and Resources, Chinese Academy of Sciences, Lanzhou 730000, China

3. College of Resources and Environment, University of the Chinese Academy of Sciences, Beijing, China 100049, China

4. College of Urban and Environmental Sciences, Northwest University, Xi'an 710069, China

5. Department of Earth Sciences, Indiana University-Purdue University Indianapolis (IUPUI), Indianapolis, IN 46202, USA

6. Forest College of Inner Mongolia Agricultural University, Hohhot, Inner Mongolia, 010018, China

7. The Key Laboratory of Mountain Environment Evolution and Regulation，Institute of Mountain Hazards and Environment, Chinese Academy of Sciences, Chengdu 610041, China

Running head: 200-year vapor-pressure deficit record

* Correspondence author:

Dr. Xiaohong LIU, E-mail: liuxh@lzb.ac.cn

State Key Laboratory of Cryosphere Sciences

Northwest Institute of Eco-Environment and Resources

Chinese Academy of Sciences

Donggang West Road 320

Lanzhou 730000, China

Tel.: +86 93-1496-7342

Abstract

Global warming will significantly increase transpirational water demand, which could dramatically affect plant physiology and carbon and water budgets. Tree-ring δ^{18}O is a potential index of the leaf-to-air vapor-pressure deficit (VPD), and therefore has great potential for long-term climatic reconstruction. Here, we developed δ^{18}O chronologies of two dominant native trees, Dahurian larch (*Larix gmelinii* Rupr.) and Mongolian pine (*Pinus sylvestris* var. *mongolica*), from a permafrost region in the Greater Hinggan Mountains of northeastern China. We found that the July-August VPD and relative humidity were the dominant factors that controlled tree-ring δ^{18}O in the study region, indicating strong regulation of stomatal conductance. Based on the larch and pine tree-ring δ^{18}O chronologies, we developed a reliable summer (July-August) VPD reconstruction since 1800. Warming growing season temperatures increase transpiration and enrich cellulose ^{18}O, but precipitation seemed to be the most important influence on VPD changes in this cold region. Periods with stronger transpirational demand occurred around the 1850s, from 1914 to 1925, and from 2005 to 2010. However, we found no overall long-term increasing or decreasing trends for VPD since 1800, suggesting that despite the increasing temperatures and thawing permafrost throughout the region, forest transpirational demand has not increased significantly during the past two centuries. Under current climatic conditions, VPD did not limit growth of larch and pine, even during extremely drought years. Our findings will support more realistic

evaluations and reliable predictions of the potential influences of ongoing climatic change on carbon and water cycles and on forest dynamics in permafrost regions.

Key words: tree-ring $\delta^{18}O$; climatic change; transpirational demand; larch; pine; Greater Hinggan Mountains

1. Introduction

The mean global temperature increased by about 0.12°C per decade from 1951 to 2012 [*IPCC* 2013]. As a result, climatic warming is expected to significantly increase the atmospheric water demand (driven by the vapor-pressure deficit, VPD) in the future [*Williams et al.,* 2013], thereby increasing the intensity of drought in forest ecosystems [*Restaino et al.,* 2016]. VPD is a function of relative humidity (RH) and temperature, and it increases with increasing temperature and decreasing RH. High VPD levels indicate high atmospheric demand for water, and plants either lose water at faster rates or close their stomata to conserve water. Because of this stomatal response, changes in VPD have important implications for ecosystem water and carbon cycling [*Kahmen et al.,* 2011*; Novick et al.,* 2016*; Restaino et al.,* 2016*; Sulman et al.,* 2016]. Thus, knowledge of long-term changes in VPD would enhance our understanding of forest water and carbon dynamics and the associated vegetation functions. However, due to the limited availability of long-term instrumental records of climatic variables in many parts of the world, proxies are often needed to infer long-term VPD trends, and to the best of our knowledge, no long-term VPD reconstruction has been published.

The oxygen stable isotope ratio (δ^{18}O) of plant cellulose has been suggested as a powerful recorder of palaeoclimatic changes [*Barbour* 2007*; McCarroll and Loader* 2004]. The δ^{18}O in tree rings reflects the integrated effects of variations in three factors: δ^{18}O in the source water, evaporative enrichment of leaf water, and biochemical fractionation during the synthesis of organic matter [*McCarroll and Loader* 2004*; Roden et al.,* 2000*; Sternberg* 2008]. Cellulose oxygen originates from oxygen in the plant's source water, which typically derives from precipitation [*Roden et al.,* 2000*; Treydte et al.,* 2014]. The δ^{18}O of precipitation is tightly correlated with climatic variables such as air temperature or the amount and geographic origin of precipitation [*Dansgaard* 1964]. Thus, plant cellulose has been proposed as an archive that can be used for reconstructing past climatic regimes and atmospheric circulation excursion [*Liu et al.,* 2014*; Saurer et al.,* 2012*; Shu et al.,* 2005*; Treydte et al.,* 2006*; Xu et al.,* 2015*; Zeng et al.,* 2016]. Another critical oxygen fractionation occurs during transpiration. Leaf water δ^{18}O values are typically enriched in ^{18}O compared with the plant's source water because evaporative losses of water from the leaves are greater for $H_2^{16}O$ than for $H_2^{18}O$ [*Roden et al.* 2000]. The enrichment of leaf water δ^{18}O may increase under drought conditions. At constant temperature, the degree of enrichment due to evaporation depends linearly on $1 - (e_a/e_i)$, where e_a and e_i are the ambient and intercellular vapor pressures, respectively [*Flanagan et al.,* 1991]. Thus, the δ^{18}O of plant cellulose is influenced by a mix of both climatic and physiological drivers.

Studies using simple correlation analyses to calibrate the δ^{18}O signal in plant cellulose have reported various relationships between plant δ^{18}O and key climatic variables such as air temperature, precipitation δ^{18}O, RH, and cloud cover [*Liu et al.,* 2014*; Rebetez et al.,* 2003*; Shu et al.,* 2005]. Due to the strong temperature-dependence of precipitation isotopes in middle- and high-latitude regions [*Dansgaard* 1964], tree-ring δ^{18}O therefore provides a reliable proxy of past changes in the growing season temperature [*Rebetez et al.,* 2003]. On the other hand, RH is important because leaf water is isotopically enriched in ^{18}O due to transpiration through plant stomata. Higher ^{18}O enrichment under dry and warm conditions (i.e., low RH) is expected, such that negative correlations exist between tree-ring δ^{18}O and RH [*Liu et al.,* 2014*; Roden et al.,* 2000*; Shu et al.,* 2005*; Xu et al.,* 2015]. In this context, such an effect might interfere with detection of temperature-dependent signals from δ^{18}O in tree rings. In a recent study, Kahmen et al. [2011] proposed that it may not be possible to determine whether air temperature or RH dominates the cellulose δ^{18}O in the absence of additional environmental information. Because of air temperature increases due to global warming, RH will likely decrease, resulting in increased evapotranspiration [*Marchin et al.,* 2016], and this may substantially alter a tree's water relations. Thus, at certain sites, by considering the combined impacts of temperature and RH, tree-ring δ^{18}O can be used as a proxy for variations in VPD [*Ferrio and Voltas* 2005*; Kahmen et al.,* 2011], because the variation of tree-ring δ^{18}O results from the simultaneous effects on δ^{18}O of the water source and leaf water evaporative loss. Over the western United States, increased temperatures have decreased tree growth significantly due to their effects on VPD [*Restaino et al.,* 2016], implying a high importance of atmospheric water demand for forest dynamics and ecosystem

water and carbon fluxes [*Novick et al.,* 2016]. In addition, a recent finding suggested that high VPD was more important than high temperature in causing a decline in tree growth [*Eamus et al.,* 2013]. These results suggest that it will be important to improve our understanding of the long-term changes in atmospheric water demand, which can be achieved using tree-ring $\delta^{18}O$ data that cover a period of several hundred years.

Boreal forests are the largest ecosystem type on Earth [*Apps et al.,* 2006], so their responses to climate change are an important concern. Recent studies have reported positive effects of climatic change on boreal forest dynamics, including increased tree growth rates due to warmer temperatures, a prolonged growing season, and the CO_2 fertilization effect, but negative responses have also been reported, such as reduced tree growth due to an increased frequency of severe weather events [*Allen et al.,* 2010*; Kharuk et al.,* 2017*; McMahon et al.,* 2010]. *Sulman et al.* [2016] revealed that high atmospheric water demand can limit forest carbon uptake, and accounted for a significant reduction of gross primary production, based on eddy-covariance and meteorological measurements. The boreal forests of northeastern China store nearly half of the country's total biomass carbon stocks [*Zhang and Liang* 2014]. Climatic change has contributed to recent increases in forest biomass throughout this region [*Zhang and Liang* 2014], and the climatic influences outweighed the importance of other disturbances. Evidence from ring width analyses of Dahurian larch (*Larix gmelinii* Rupr.) and Mongolian pine (*Pinus sylvestris* var. *mongolica*) also indicated a recent increase in their growth rate [*Zhang et al.,* 2017], which may have resulted from warming and an increase of the thaw depth in the region's permafrost. In contrast, *Bao et al.* [2014] reported that growth of the pine was strongly limited by seasonal drought and has declined recently. These distinct

climatic responses of tree growth may be species- or site-specific. To reconcile these contrasting responses of tree growth to climatic change, tree-ring $\delta^{18}O$ can provide additional information from a physiological point of view that reveals tree responses to recent climatic changes.

In the present study, we used tree-ring samples from the dominant Dahurian larch and Mongolian pine growing in the permafrost region of northeastern China to determine the climatic significance of tree-ring $\delta^{18}O$. Then, based on the statistically significant relationships and mechanistic and physiological knowledge, we established a robust VPD reconstruction since 1800 to present for the study region. We further evaluated the possible linkages between VPD and tree growth of the larch and pine since 1800. We hypothesized that the increasing temperature throughout the study region would increase plant transpirational water demand, thus increasing stomatal water loss and resulting in higher $\delta^{18}O$ values in the tree rings. For a species with strong stomatal regulation in response to climatic change, the potential signal from the water source $\delta^{18}O$, which is related to temperature, would be hidden by the strong variability in transpirational enrichment, making it feasible to reconstruct VPD based on tree-ring $\delta^{18}O$. Our estimated VPD series will help to reduce the uncertainties of ecosystem models that simulate the long-term fluxes and states of water and carbon.

2. Materials and Methods

2.1. Study area

The Greater Hinggan Mountains (Figure 1a) lie in a region with a typical semi-humid continental monsoon climate in northeastern China. The annual mean temperature is -3.9°C, with monthly mean temperatures ranging from 17.3 °C in July to -28.1°C in January (Figure 1b). All of the temperature parameters (mean, maximum, and minimum temperatures) have shown a significant increasing trend from 1957 to 2013 (Figure S1 a-c), with relatively flat trends since 1990. The monthly mean precipitation from June to August accounted for 67.0% of the mean annual precipitation, which averaged 473.5 mm from 1957 to 2013 (Figure 1c); the total ranged from 324.4 mm in 1986 to 764.4 mm in 2013 (Figure S1). Precipitation, RH, and VPD all peak during the growing season (Figure 1c). The total annual precipitation shows a marginally significant increasing trend from 1957 to 2013, but with an unusually flat extreme peak in 2013. Because of the increasing air temperature, yearly RH has decreased significantly during this period (Figure S1e). The calculated standardized precipitation-evapotranspiration index (SPEI) showed no significant trend (Figure S1f). However, VPD has increased significantly during this period (Figure S1g).

The Xing'an-Baikal permafrost in our study area is the second-largest permafrost area in China, and represents high-latitude permafrost because it occurs at latitudes greater than 47°N. In response to global warming, the thawing depth to the permafrost has increased steadily, at a rate of 9 cm per decade based on data from the Jiagedaqi District weather station from 1960 to 2010, and the permafrost area has retreated northward by 50 to 150 km during the past 50 years [*Jin et al.,* 2000*; Cheng and Jin* 2013]. Soil moisture in the permafrost's

active layer has decreased due to disruption of the permafrost, leading to increased drainage; as a result, the rooting layer often lacks sufficient moisture to support optimal plant growth [*Wang and Song* 2011].

The dominant tree species in the Greater Hinggan Mountains are Dahurian larch and Mongolian pine, which are adapted to the harsh permafrost environment, even though the frozen soils limit tree growth. The growing season for trees in this region lasts from the end of May to the beginning of September [*Fu et al.,* 2016]. The stands at our sampling sites are growing in flat terrain. The main soils are acidic or subacidic luvisols, sometimes with a thin surface layer of mineral soil or wind-blown sandy soil. Mongolian pine and Dahurian larch forests are always mixed with small amounts of *Picea jezoensis*, *Abies nephrolepis*, and *Pinus koraiensis* [*Wang and Song* 2011].

2.2. Tree-ring sampling

We sampled a total of 234 tree cores (two cores per tree, obtained at right angles) at breast height using 12-mm-diameter increment borers in October 2013. The samples came from 72 Dahurian larch trees (27 from site 1, 21 from site 2, and 24 from site 3), and 45 Mongolian pine trees (24 from site 1 and 21 from site 2) without obvious damage or disturbance (Table S1). We measured tree-ring widths using a LINTAB 6 measuring system (http://www.rinntech.de) with a resolution of 0.01 mm. We used the COFECHA software (http://www.ldeo.columbia.edu/tree-ring-laboratory/resources/software) to control the quality of the cross-dating, and the ARSTAN software (http://www.ldeo.columbia.edu/tree-ring-laboratory/resources/software) to develop site chronologies.

The length of the ring-width chronologies at the five sampling sites ranged from 224 years at larch site 3 to 347 years at pine site 2 [*Zhang et al.,* 2017]. The mean sensitivity of the larch width chronologies was greater than 0.26; the mean sensitivity of the pine chronologies was lower, but still greater than 0.20 (Table S1). The inter-series correlations (RBAR) among the three larch ring-width chronologies were all greater than 0.59 ($P < 0.001$, period from 1780 to 2013), whereas the RBAR values for pine were 0.56 ($P < 0.001$, period from 1683 to 2013) (Table S1). The relatively strong correlations and regional coherence suggest that common factors affected the growth variability of larch and pine. Based on the species-specific data for the common period at all sites, we developed species chronologies from 1780 to 2013 and used them to represent the regional tree-ring width chronologies for Dahurian larch and Mongolian pine. The constructed larch and pine tree-ring width index chronologies covered the period of 1722-2013 and 1666-2013, respectively. Based on the EPS value (>0.85), the robust periods of ring width chronologies were 1850-2013 and 1770-2013 for larch and pine, respectively [*Zhang et al.,* 2017].

2.3. Cellulose extraction and δ^{18}O analysis

We selected five cores (one core per tree) for each species that had homogeneous growth patterns and pooled the annual wood samples for a given species, without considering the relative contributions of earlywood and latewood mass, prior to α-cellulose extraction. In this step, we ensured each sampling site (Table S1) had at least one core into the species-specific isotope time series. This follows the results from earlier studies, which suggested that four or five tree-ring cores are required for stable oxygen isotope analyses to

represent the environmental conditions at a specific site [*Shi et al.,* 2011] and that the

mass-biased influence on isotopes within a single tree ring can be ignored [*Leavitt* 2008*; Liu et al.,* 2015]. We discarded the initial 20 years of the samples to avoid potential juvenile

effects [*Liu et al.,* 2014*; Xu et al.,* 2015]. In addition, we pooled the samples for a given

species because several tree-ring $\delta^{18}O$ studies [*Liñán et al.,* 2011*; Szymczak et al.,* 2012] have

suggested that pooling without considering the contributions of individual trees to the pooled

chronology produces a site $\delta^{18}O$ chronology that corresponds well to a chronology based on

the mean values calculated from analyses of individual trees. We milled the pooled annual

samples and then extracted α-cellulose using the methods of *Loader et al.* [1997]. To better

homogenize the cellulose, we used an ultrasound machine (JY92-2D,

http://www.scientzbio.com/) to break the cellulose fibers, following the method of *Laumer et al.* [2009].

For the oxygen isotope measurements, we weighed the dry α-cellulose samples (0.14

to 0.16 mg) in silver capsules. We measured the isotope ratio ($^{18}O/^{16}O$) with a

High-Temperature-Conversion Elemental Analyzer (TC/EA) at 1350°C coupled to a Finnigan

MAT-253 mass spectrometer at the Northwestern Institute of Eco-Environment and

Resources, Chinese Academy of Sciences. The $\delta^{18}O$ analyses were repeated four times for

each annual cellulose sample. In all analyses, we used the mean isotopic values of each

sample. The mean standard deviation of the replicated samples was lower than 0.20‰ for the

four repeated measurements [*Liu et al.,* 2014*; Xu et al.,* 2015]. We used a cellulose standard

(IAEA-C$_3$; 32.2‰) and commercial cellulose (Fluka Analytical,

www.sigmaaldrich.com/germany.html; 28.2‰) to calibrate the measurements of tree-ring

δ^{18}O cellulose. In the following analysis, we mainly focused on the period from 1800 to 2010, when δ^{18}O in tree rings of both tree species were measured.

2.4. Climate variables

Climate data were obtained from the China Meteorological Administration (http://www.cma.gov.cn/en/). Monthly precipitation, the mean maximum, minimum, and mean monthly temperatures, and RH were obtained from three meteorological stations near to the sampling sites (Xinlin, Tulihe, and Genhe; Figure 1a). Regional meteorological data were produced by averaging the monthly records for the period when data was available for all three stations, from 1957 to 2013. We also used the standardized precipitation-evapotranspiration index (SPEI), a multiscalar drought index that combines the effects of precipitation and potential evapotranspiration [*Vicente-Serrano et al.,* 2010] to quantify thermo-water demand of trees. Values of SPEI greater than the long-term mean for a region indicate wetter moisture conditions, and values lower than the long-term mean indicate drier conditions. We calculated monthly SPEI values according to the method of *Vicente-Serrano et al.* [2010]. The monthly VPD values were estimated by the method of *Hogg* [1997] and *Hogg et al.* [2013]. The mean VPD can be estimated from the saturation vapor pressure (kPa) at the monthly mean values of daily maximum temperature ($e^*_{T\max}$), minimum temperature ($e^*_{T\min}$), and dewpoint temperature ($e^*_{T\text{dew}}$):

$$\text{VPD} = 0.5 \times \left(e^*_{T\max} + e^*_{T\min}\right) - e^*_{T\text{dew}} \qquad (1)$$

Where e^*_T represents the relationship between air temperature (T, °C) and saturated vapor pressure, $e^*_T = e_0 \times 10^{\left(\frac{7.5T}{T+237.3}\right)}$, the value of e_o was 0.611 kPa, and T was the mean monthly temperature. Mean monthly T_{dew} was estimated as the saturation vapor pressure at the

monthly mean value of T_{min} minus 2.5°C [*Hogg,* 1997]. The monthly temperature and precipitation from the nearest four cells in the CRU grid (Figure 1a; http://www.cru.uea.ac.uk/) were also extracted and averaged to characterize the regional July-August temperature and precipitation from 1901 to 2010 and examine the possible long-term driving forces for VPD.

2.5. Statistical analysis

We looked for statistically significant relationships between tree-ring $\delta^{18}O$ and the climatic variables (monthly mean temperature, monthly mean maximum and minimum temperatures, monthly precipitation, monthly RH, SPEI, and VPD) by performing correlation analyses (using Pearson's r) to quantify the climate–$\delta^{18}O$ relationships based on data from the previous October to the current October. All statistical calculations were performed using version 18.0 of the SPSS software (http://www.ibm.com/analytics/us/en/technology/spss). To evaluate the connections between the $\delta^{18}O$ chronologies for the two species over time, we used a 21-year sliding-window correlation. To confirm the influence of the climatic parameters on tree-ring $\delta^{18}O$, we calculated the correlations between $\delta^{18}O$ and the climatic variables for both annual values and the first-order differences. To account for the decrease in ring width that occurs with increasing tree size, we converted each ring's radial increment into a basal area increment (BAI) using the following formula [*Biondi and Qeaden,* 2008]:

$$BAI = \pi\,(R^2_n - R^2_{n-1}) \quad (2)$$

where R is the radius of the mean ring width from all trees that had distinct growth rings in a given year and n is the year of tree-ring formation. Unlike a raw ring-width series, BAI minimizes the effect of tree size and age on annual growth trends while retaining the high-

and low-frequency signals contained in the tree-ring series [*Biondi and Qeaden,* 2008]. As the tree growth (BAI) showed clear trends (Supplementary Figure S3), with an initial increase for the young tree followed by a decrease as the tree ages, we calculated the correlations between the residuals of a second-order polynomial fit for the BAI data from 1800-2010 and the reconstructed VPD. Moreover, we performed correlation analyses between VPD and tree growth for the annual data and first-order differences to explore the possible linkages between the two parameters.

3. Results

3.1. Tree-ring $\delta^{18}O$ records of larch and pine

The larch $\delta^{18}O$ series covered the period from 1800 to 2010, and the pine $\delta^{18}O$ series covered the period from 1730 to 2013. The mean $\delta^{18}O$ values of larch and pine during the common period from 1800 to 2010 were 23.8 ± 0.87‰ and 25.6 ± 1.16‰, respectively, with an overall mean $\delta^{18}O$ enrichment of 1.79‰ for the pine tree rings. $\delta^{18}O$ chronologies of the two species during the common period from 1800 to 2010 (Figure 2a) were significantly positively correlated ($r = 0.63$, $p < 0.05$). The 21-year sliding-window correlation showed weaker correlations between the larch and pine $\delta^{18}O$ series in the earliest and most recent 20-year periods, which corresponded to high variability in the $\delta^{18}O$ difference between the two tree species (Figure 2b). However, during the common period from 1950 to 2010, the $\delta^{18}O$ series for larch and pine remained highly coherent ($r = 0.52$, $P < 0.001$).

3.2. Climatic controls of tree-ring $\delta^{18}O$

The correlations between tree-ring $\delta^{18}O$ and the climatic parameters (maximum temperature, RH, and VPD) had similar patterns for larch and pine (Table S2). The climatic response analyses revealed stronger correlations between tree-ring $\delta^{18}O$ and moisture conditions than between $\delta^{18}O$ and temperature. The most important months were during the current growing season (but particularly in July and August). For the annual variation, larch $\delta^{18}O$ was also significantly negatively correlated with the RH before the growing season (from the previous December to the current March), but these correlations were not significant for the high-frequency (first-order) variations, possibly as a result of removing the low-frequency variations in both series (Table S2). In addition, compared to RH and VPD, precipitation and SPEI had fewer significant correlations with $\delta^{18}O$ for both larch and pine. If we combine the annual and high-frequency variations for the relationships between tree-ring $\delta^{18}O$ and the climatic parameters, the results strongly indicate that the mean July-August maximum temperature, RH, and VPD strongly influence tree-ring $\delta^{18}O$ (Table S3).

We plotted the temporal trends of $\delta^{18}O$ against the three significant parameters: mean July-August maximum temperature, RH, and VPD (Figure 3, 4). For the yearly variations, RH and VPD had stronger relationships (higher R^2) than temperature with tree-ring $\delta^{18}O$ for both larch and pine, indicating stronger stomatal regulation on evaporative enrichment of leaf water [*McCarroll & Loader*, 2004]. The high-frequency variations represented by the first-order difference confirmed the dominant control of stomatal conductance by moisture conditions (Figure 4), and therefore stomatal control of cellulose $\delta^{18}O$. A systematic increase of $\delta^{18}O$ in the tree-ring chronology may result from increasing air temperature or decreasing

RH. As a consequence, the combined effects of RH and air temperature on cellulose $\delta^{18}O$ can be integrated into a single environmental index of the atmospheric water deficit (i.e., VPD) for trees. This is supported by the stronger correlations between tree-ring $\delta^{18}O$ and VPD (Figure 3, 4).

3.3. VPD reconstruction

We combined the tree-ring $\delta^{18}O$ series for larch and pine to reconstruct the growing season (July-August) VPD using a linear regression model based on the $\delta^{18}O$ and VPD dataset from 1957 to 2010. The reconstructed and actual VPD showed highly coherent changes and strong relationship during the common period from 1957 to 2010 (Figure 5a). After removing an outlier (in 1971), the model explained about 56.1% of the total variance ($P < 0.001$; Figure 5b). We evaluated the model's validity using a standard split-calibration and independent verification approach for the periods from 1957 to 1984 and from 1985 to 2010 (Table 1). The reduction of error (RE), coefficient of efficiency (CE), leave-one-out test, and sign test demonstrated that the transfer function was stable and reliable. The two more rigorous tests (RE and CE) were both positive (Table 1), which confirms the validity of the regressions and the suitability of our time series for climate reconstruction. In addition, we compared the reconstructed July-August VPD based on either the combination of both tree species or on pine alone (Figure 5c). The comparison showed that the reconstructed VPD based on the two tree species had a wider range, suggesting a stronger ability to record extreme events for the combination of both tree species than for that based on pine alone. Our results also revealed a decreasing trend in the reconstructed VPD time series from 1730 to 1840 (Figure 5c), which indicates a change in atmospheric water demand from relatively dry

to relatively wet during this period.

We then used the KNMI Climatic Explorer software (http://www.knmi.nl) to explore the spatial correlation of the temperature and precipitation with the reconstructed July-August VPD during the periods from 1901 to 1956 and from 1957 to 2010, respectively (Figure 6). The spatial patterns showed that our reconstruction was significantly and positively correlated with temperatures southwest of the study area both from 1901 to 1956 and from 1957 to 2010 (Figure 6a,b). Our results also suggest that the reconstructed VPD based on observed meteorological data from 1957 to 2010 (Figure 6b) was stronger over a wider area than that inferred from the interpolated CRU data before 1956 (Figure 6a). For precipitation, our reconstructed VPD series was most strongly correlated with precipitation recorded in the study area both from 1901 to 1956 (Figure 6c) and from 1957 to 2010 (Figure 6d). This also suggests that in the permafrost region of northeastern China, local precipitation was more important than local temperature for the water-energy balance.

Based on our reconstruction of the July-August VPD, we found no significant long-term trend since 1800 (Figure 7a). The periods with the highest atmospheric water demand occurred between 1914 and 1926, followed by three periods (1855 to 1860, 1940-1950 and 2001 to 2006) with relatively higher values. The lowest VPD occurred in 1846. The recent warming (since 1957) also corresponded to a period with gradually increased VPD, although VPD did not exceed the peak values around 1920.

4. Discussion

4.1. Coherence of tree-ring δ^{18}O series between tree species

Several studies confirmed that tree-ring δ^{18}O shows large-scale coherence between species [*Baker et al.,* 2015*; Liu et al.,* 2014], and the authors proposed that this coherence was probably caused by a strong spatial coherence in precipitation δ^{18}O due to the large-scale controls on this property. Based on the precipitation δ^{18}O data from GNIP stations and IAEA, spatial variation of precipitation δ^{18}O over China has been estimated [Liu et al., 2008]. We found precipitation δ^{18}O was within anarrow range (about -14~-12‰) in our study area [*Liu et al.*, 2008]. The present larch and pine δ^{18}O chronologies also showed strong coherence since 1800 (Figure 2a), suggesting the existence of at least two common drivers for tree-ring δ^{18}O of the two species. We hypothesize that the first likely arises from a dominant imprint of interannual variation in precipitation δ^{18}O on tree-ring δ^{18}O via a strong influence of the water source δ^{18}O [*Baker et al.,* 2015*; Liu et al.,* 2014]. The second is leaf water enrichment, which may dampen the effect of variations in water source δ^{18}O [*Ferrio and Voltas* 2005*; Kahmen et al.,* 2011*; Treydte et al.,* 2014]. At most times, the mixed signals from the water source and leaf water enrichment are difficult to separate completely. Considering the similar precipitation δ^{18}O values over the northern Great Hinggan Mountains [*Liu et al.*, 2008], the offset in the mean values of δ^{18}O between the two species (Figure 2b) may have resulted from species-specific differences in the root distribution and transpiration rate. Root depth structure difference between species (i.e., spatial partitioning) affects the water-source δ^{18}O due to the existence of isotopic gradients in soil water, with heavier isotopes becoming depleted in deeper soil [*Tang and Feng,* 2001; *Sarris et al.,* 2013].

Due to the proximity and similar topographic feature among our sampling sites, the water source is similar and likely derives from precipitation for the two tree species. Thus, the deeper rooting of larch would lead to less tree-ring ^{18}O enrichment than in pine (Figure 2b; Sidorova et al., 2016). Species-specific physiological differences may also explain some of the variability between the tree-ring δ^{18}O records. Pine is evergreen and larch is deciduous, which will influence the earlywood δ^{18}O values due to differences in the degree of utilization of previously stored carbohydrates. In addition, interspecies variation in the responses of transpiration to changes in RH (Figure 3b,e) may affect the degree to which differences resulting from variation in source water δ^{18}O are maintained in tree-ring δ^{18}O. Recently, *Sidorova et al.* [2016] found that tree-ring δ^{18}O in larch (*Larix decidua*) and pine (*Pinus mugo* var. *uncinata*) growing in a Swiss national park showed different dependence on RH and precipitation δ^{18}O. We considered that differential physiological responses of two tree species to seasonal climatic changes is reasonable in our study.

The isotopic exchange during cellulose synthesis between the carbohydrates and the medium water of each tree species will further alter the signal from leaf water enrichment [*Roden et al.,* 2000*; Song et al.,* 2014]. The magnitude of this exchange is positively related to the time between carbohydrate production in the leaf and cellulose synthesis in the stem (i.e., the carbohydrate turnover time; *Song et al.,* [2014], which may itself vary considerably between species. Yet, the detailed information about exchange rate between species over growth season is still unknown for larch and pine over the study region.

The recent divergence of the δ^{18}O correlation between larch and pine since 1980 (Figure 2b) is likely the result of differences in the species-specific physiological responses to changes in the water–energy balance caused by climate warming. *Sidorova et al.* [2009] reported a clear change in tree-ring δ^{18}O and climate trends after the 1960s, and suggested that it was a response of trees to water deficits during the last half century in permafrost in northern Siberia. They argued that melting permafrost water is highly depleted in ^{18}O and could therefore cause decreasing tree-ring δ^{18}O trends. Recently, *Saurer et al.* [2015] proposed a conceptual framework that described the negative feedback between drought and the water source δ^{18}O and therefore the effect on tree-ring δ^{18}O values of larch. However, there have been no water isotope observations in the permafrost soil profile of our study region, we cannot determine whether the recent increases in the depth of permafrost thawing and the resulting mixing of water sources have contributed to recent decreases in the correlations between the tree-ring δ^{18}O of larch and pine. To clarify the reasons for this divergence, additional information will be required about soil hydrology in permafrost regions [*Saurer et al.,* 2015; *Fedorov et al.*, 2017] and about tree physiological adaptations to recent climatic change.

4.2. Climatic significance of tree-ring δ^{18}O

Because many variables can affect the δ^{18}O values of precipitation [*Dansgaard,* 1964*; Dayem et al.,* 2010*; Johnson and Ingram,* 2004; *Liu et al.,* 2010], it is difficult to understand which environmental signals are ultimately recorded in plant cellulose δ^{18}O. When plants use precipitation as their primary water source, the precipitation δ^{18}O signal will transfer directly into the plant cellulose. Precipitation δ^{18}O in our study region was mainly controlled by

temperature based on analyses of the spatial distribution of δ^{18}O over China [*Johnson and Ingram,* 2004*; Zhao et al.,* 2012]. Thus, tree-ring δ^{18}O of larch and pine may partially reflect the effects of temperature variations. This is consistent with the positive correlations between temperature and δ^{18}O in the tree rings of both species (Table S2). However, this temperature signal will be altered by the leaf water enrichment that occurs through leaf responses to VPD changes. About 50% of the oxygen atoms with enrichment signal will be further exchanged with xylem water [*Roden et al.,* 2000], thereby mixing the effects of water source δ^{18}O with those of leaf-level enrichment. In some cases, the source water δ^{18}O signal in tree-ring δ^{18}O decreases in strength when water is limiting and VPD increases [*Ferrio and Voltas,* 2005]. Thus, the water-source related temperature-δ^{18}O signals cannot be separated without additional information.

The association between δ^{18}O in tree rings and moisture conditions was stronger than the association with temperature (Table S2), suggesting that tree-ring δ^{18}O variations were more closely related to transpirational demand than to the temperature signal related to precipitation δ^{18}O [Liu et al., 2009]. The different strengths of the relationships between tree-ring δ^{18}O and the moisture conditions (precipitation/SPEI and RH/VPD) also indicate the existence of an independent constraint on tree-ring δ^{18}O of larch and pine, created by the soil moisture supply and atmospheric water demand. This suggests that atmospheric water demand plays a stronger role than temperature on oxygen isotope fractionation in cold and wet regions such as our study area. Although tree-ring δ^{18}O was strongly correlated with RH from the previous December to the current March for larch and with RH and VPD from the previous September and October for pine based on the annual variations, the first-order

difference analysis did not show these correlations. This suggests that these associations with the climate during the previous growing season are not real. Our results are consistent with results in northern Siberia, where larch tree-ring $\delta^{18}O$ were regulated by temperature and VPD [*Sidorova et al.,* 2009]. As suggested by *Kahmen et al* [2011], by combining the individual impacts of temperature and RH together, we reconstructed the July-August VPD changes since 1800. Calibration and verification statistics confirmed that our reconstruction was robust and reliable (Table 1).

4.3. VPD trends and driving forces

We compared the reconstructed July-August VPD with the corresponding CRU VPD from 1901 to 2010 (Figure S2). Both series changed synchronously and showed good coherence in their extreme values, but there was an overall offset of 0.17 kPa, with the reconstructed VPD being lower than the CRU VPD. The highest values in the reconstructed VPD series occurred during the 1920s, and this peak was not evident in the CRU VPD series. The two VPD series were significantly correlated ($r = 0.56$, $p < 0.05$) from 1901 to 2010 (Figure S2b), confirming that our reconstruction and the CRU VPD series share a common forcing. The overall offset between the reconstructed and CRU VPD series may have resulted from differences in the temperature parameters between the observed and interpolated CRU data (Table S4). This provides a reminder that the CRU data must be calibrated based on local observations before it can be used to evaluate regional climatic change.

We compared the long-term trends of the reconstructed July-August VPD and the July-August CRU temperature and precipitation values to explore the potential driving factors for VPD (Figure S3). The overall correlation between VPD and temperature was

positive and significant ($P = 0.008$, 1901 to 2010), and the slope of the temperature–VPD

relationship was 0.022 kPa/°C (Figure S3b). For July-August precipitation, the correlation

was much stronger but negative, with $R^2 = 0.276$ and a rate of -0.98 kPa/100 mm (Figure

S3d), suggesting that for the study region, the impact of changes in precipitation on

atmospheric water demand was more important than that of temperature. Overall, we found

no statistically significant trend of increasing VPD in the study region. This is consistent with

the projection based on a general circulation model that there will be only a limited increase

of VPD at high latitudes during the 21st century [*Cook et al.,* 2014].

4.4. Tree-growth and atmospheric water demand

VPD changes will affect stomatal conductance and therefore the flow of water vapor in forest

ecosystems. During dry conditions, the stomata close to conserve water, whereas under wet

conditions the stomata open to optimize CO_2 assimilation. A statistical model based on

long-term eddy covariance measurements highlighted the importance of VPD as a component

of drought and as a driver of carbon and water fluxes under well-watered conditions [*Sulman*

et al., 2016]. In forests of the western United States, there is evidence indicating that

increased temperatures have decreased tree growth via the resulting increase in VPD

[*Restaino et al.,* 2016]. Here, we evaluated the correlations between BAI of larch and pine

and the reconstructed VPD since 1800. The BAI of both species increased from 1800 to 1927,

and then decreased until 1990 (Figure S4c). By examining Figure S4c more closely, an

increase in tree growth appears to have begun in 1990; this increase was statistically

significant for both species ($R^2 = 0.13$ for larch ($P = 0.10$), $R^2 = 0.40$ ($P < 0.01$) for pine). The

recovery of tree growth is consistent with the increase in VPD since 1990. This can be

supported by the results from *Zhang et al.* [2016] who reported that the recent warming that has occurred since 1957 would benefit tree radial growth in the high-latitude permafrost zone due to the increasing depth of permafrost thawing. As a result, the acceleration of thawing of the permafrost will alter the water-source conditions and the thermal and moisture conditions in the soil environment, which will therefore affect the cellulose $\delta^{18}O$. In addition, the extended growing season throughout the region will also improve tree growth [*Fu et al.,* 2016]. We found slight trends for the relationship between VPD and BAI of both tree species based on the yearly variations; however, the linear regressions were not significant (Larch: $y = 6.21x + 6.65$, $R^2 = 0.08$, *ns*; Pine: $y = 4.07x + 5.56$, $R^2 = 0.08$, *ns*) (Figure S4a). For the high-frequency variations representing the first-order difference calculation, VPD significantly and positively influenced larch growth ($y = 8.10x + 0.033$, $R^2 = 0.0056$, $P < 0.01$) (Figure S4b), but the relationship was not significant for pine ($y = 0.099x + 0.025$, $R^2 = 0.0004$, *ns*). Figure S4c shows clear low-frequency variations (second-order quadratic equation) in the BAI of larch and pine, which represents biological effects on tree growth. Hence, we used an alternative method to examine the long-term relationships between tree growth and VPD. We applied polynomial regression to remove the effects of these low-frequency variations. The relationships between the residual BAI and the reconstructed BAI showed a significant positive influence of VPD on tree growth (both $P < 0.05$), although the strength of the relationship was weak (Figure S4d). We also checked the correlations between VPD and tree growth deduced by traditional standard tree-ring width in the common period, and reached the same conclusions (Figure not provided).

To confirm the long-term contributions of VPD and BAI, we examined the correspondence between years with extreme values. Here, we defined "extreme" to mean VPD values more than one standard deviation (SD) from the mean; if the VPD value was greater than mean+1SD, we defined that year as representing a drought, whereas when VPD was less than mean−1SD, we defined that as a wet year (Figure 7a). On this basis, we identified 33 drought years and 30 wet years since 1800. For the wet years (Figure 7b, c, d), there was no significant relationship between VPD and BAI based on both the yearly and the first-order difference variations for both tree species ($P > 0.05$). However, for drought years, with higher atmospheric demand, VPD significantly and positively affected growth in pine based on the yearly variations ($R^2 = 0.119$, $P = 0.049$) (Figure 7e). For the high-frequency variations, the responses of BAI to VPD were all positive, but the relationship was not significant for tree growth ($R^2 = 0.116$ and $R^2 = 0.075$, $P > 0.05$) (Figure 7e, f, g). Above results suggested no significant limitations of increased VPD on tree growth. Overall, our results differ from previous reports that suggested that increased VPD would decrease plant growth under the recent warming trend [*Restaino et al.,* 2016*; Sulman et al.,* 2016].

5. Conclusions

We developed a VPD reconstruction since 1800 for a permafrost area within the Greater Hinggan Mountains of northeastern China based on the tree-ring $\delta^{18}O$ record of larch and pine. The reconstruction accounted for 56.1% of the total variance during the calibration period from 1957 to 2010. There was no significant long-term trend in the reconstructed VPD

since 1800. The period with the most severe atmospheric water demand occurred from around 1915 to 1924, with high variability in VPD from 1850 to 1950. The July-August VPD showed an increasing trend following the warming that has been observed since 1960. By comparing the BAI of larch and pine with the reconstructed VPD series, we revealed that the atmospheric water demand did not limit tree growth despite the continuous warming that has occurred in this permafrost forest. Overall, our tree-ring $\delta^{18}O$ series provided an effective proxy for plant physiology, independent of the traditional ring-width series. To obtain a more robust assessment of the contribution of atmospheric water demand to tree growth in this specific high-latitude permafrost environment, further evidence from eddy covariance studies [*Sulman et al.,* 2016] and physiological measurements [*Marchin et al.,* 2016] will be needed.

Acknowledgments

References

Allen, C.D., Macalady, A.K., Chenchouni, H., Bachelet, D., McDowell, N., Vennetier, M., Kitzberger, T., Rigling, A., Breshears, D.D., Hogg, E.H.T., Gonzalez, P., Fensham, R., Zhang. Z., Castro, J., Demidova, N., Lim, J., Allard, G., Running, S.W., Semerci. A., Cobb, N. (2010), A global overview of drought and heat-induced tree mortality reveals emerging climate change risks for forests. *Forest Ecol. Manag.,* 259, 660-684

Apps, M.J., Shvidenko, A.Z., Vaganov, E.A. (2006), Boreal forests and the environment: a foreword, mitigation and adaptation strategies for global change. *Mitig. Adapt. Strat. Glob. Change,* 11(1), 1-4.

Baker, J., Hunt, S.F.P., Clerici, S., Newton, R.J., Bottrell, S.H., Leng, M.J., Heaton, T.H.E., Helle, G., Argollo, J., Gloor, M., Brienen, R.J.W. (2015), Oxygen isotopes in tree rings show good coherence between species and sites in Bolivia. *Glob. Plane Change,* 133, 298-308

Bao, G., Liu, Y., Liu, N., Linderholm, H.W. (2014), Drought variability in eastern Mongolian Plateau and its linkages to the large-scale climate forcing. *Clim. Dyn.,* 44, 717-733. doi: 10.1007/s00382 -014-2273-7

Barbour, M.M. (2007), Stable oxygen isotope composition of plant issue: a review. *Func. Plant Biol.,* 34, 83-94

Biondi, F., Qeaden, F. (2008), A theory-driven approach to tree-ring standardization: defining the biological trends from expected basal area increment. *Tree-ring Res.,* 64, 81-96

Cheng, G., Jin, H. (2013), Permafrost and groundwater on the Qinghai-Tibet plateau and in

northeast China. *Hydrogeol. J.,* 21(1), 5-23.

Cook, B.I., Smerdon, J.E., Seager, R., Coats, S. (2014), Global warming and 21st century drying. *Clim. Dyn.,* 43, 2607-2627.

Dansgaard, W. (1964), Stable isotopes in precipitation. *Tellus,* 14, 436-468

Dayem, K,E,, Molnaar, P., Battisti, D.S., Roe, G.H. (2010), Lessons learned from oxygen isotopes in modern precipitation applied to interpretation of speleothem records of paleoclimate from eastern Asia. *Earth Planet Sci. Lett.,* 295, 219-230

Eamus, D., Boulain, N., Cleverly, J., Breshears, D.D. (2013), Global change-type drought-induced tree mortality: vapor pressure deficit is more important than temperature per se in causing decline in tree health. *Ecol. Evol.*, 3(8), 2711–2729, doi: 10.1002/ece3.664

Fedorov, A.N., Iwahana, G., Konstantinov, P.Y., Machimura, T., Argunov, R.N., Efremov, P.V., Lopez, L.M.C., Takakai F. (2017), Variability of permafrost and landscape conditions following clear cutting of larch forest in central Yakutia. *Permafrost Periglacial Proce.* 28, 331-338

Ferrio, J.P., Voltas, J. (2005), Carbon and oxygen isotope ratios in wood constituents of *Pinus halepensis* as indicators of precipitation, temperature and vapour pressure deficit. *Tellus*, 57B, 164-173

Flanagan, L.B., Comstock, J.P., Ehleringer, J.R. (1991), Comparison of modeled and observed environmental influences on the stable oxygen and hydrogen isotope composition of leaf water in *Phaseolus vulgaris* L. *Plant Physiol.*, 96, 588-596

Fu, Y.Y., Zhao, J.J., Zhang, H.Y., He, H., Guo, X. (2016), Spatiotemporal variation of

vegetation phenology in the Daxing'an Mountains stratified by ecogeographical regions. *Chinese J Applied Ecol.*, 27(9), 2797-2806

Hogg, E.H. (1997), Temporal scaling of moisture and the forest–grassland boundary in western Canada. *Agri. Forest Meteorol.,* 84, 115-122

Hogg, E.H., Barr, G., Black, T.A. (2013), A simple soil moisture index for representing multi-year drought impacts on aspen productivity in the western Canadian interior. *Agri. Forest Meteorol.,* 178,173-182

IPCC, (2013), *Summary for Policymakers.* In: *Climate Change 2013*: Stocker, T.F., Qin, D., Plattner, G.-K., Tignor, M., Allen, S.K., Boschung, J., Nauels, A., Xia, Y., Bex, V., Midgley P.M., et al., The Physical Science Basis. Contribution of Working Group I to the Fifth Assessment Report of the Intergovernmental Panel on Climate Change Cambridge University Press, Cambridge.

Jin, H., Li, S., Cheng, G., Wang, S.L., Li. X. (2000), Permafrost and climatic change in China. *Glob. Plane Change*, 26, 387-404

Johnson, K.R., Ingram, B.L. (2004), Spatial and temporal variability in the stable isotope systematics of modern precipitation in China. Implications for paleoclimate reconstruction. *Earth Planet Sci. Lett.,* 220, 365-377

Kahmen, A., Sachse, D., Arndt, S.K., Tu, K.P., Farrington, H., Vitousek, P.M. (2011), Cellulose δ^{18}O is an index of leaf-to-air vapor pressure difference (VPD) in tropical plants. *Proc. Natl. Acad. Sci. USA,* 108(5), 1981-1986

Kharuk, V.I., Im, S.T., Petrov, I.A., Golyukov, A.S., Ranson, K.J., Yagunov, M.N. (2017), Climate-induced mortality of Siberian pine and fir in the Lake Baikal Watershed, Siberia.

Forest Ecol. Manag., 384: 191-199

Laumer, W., Andreu, L., Helle, G., Schleser, G.H., Wieloch, T., Wissel, H. (2009), A novel approach for the homogenization of cellulose to use micro-amounts for stable isotope analyses. *Rapid Commun. Mass Spectrom.,* 23(13), 1934-1940. doi: 10.1002/rcm.4105.

Leavitt, S.W. (2008), Tree-ring isotopic pooling without regard to mass: no difference from averaging $\delta^{13}C$ values of each tree. *Chem. Geol.,* 252, 52-55

Liñán, I.D., Gutiérrez, E., Helle, G., Heinrich, I., Andreu-Hayles, L., Planells, O., Leuenberger, M., Burger, C., Schleser, G. (2011), Pooled versus separate measurements of tree-ring stable isotopes. *Sci. Total Environ.*, 409(11), 2244-2251.

Liu X., An, W., Treydte, K., Wang, W., Xu, G., Zeng, X., Wu, G., Wang, B., Zhang, X. (2015), Pooled versus separate tree-ring δD measurements, and implications for reconstruction of the Arctic Oscillation in northwestern China. *Sci. Total Environ.*, 511, 584-594

Liu, X., Xu, G., Grießinger, J., An, W., Wang, W., Zeng, X., Wu, G., Qin, D. (2014), A shift in cloud cover over the southeastern Tibetan Plateau since 1600: evidence from regional tree-ring $\delta^{18}O$ and its linkages to tropical oceans. *Quat. Sci. Rev.,* 88, 55-68

Liu, Z., Tian, L., Chai, X., Yao, T. (2008), A model-based determination of spatial variation of precipitation $\delta^{18}O$ over China. *Chem. Geol.,* 249(1-2), 203-212

Liu, Z., Bowen, G.J., Welker, J.M. (2010), Atmospheric circulation is reflected in precipitation isotope gradients over the conterminous United States. *J. Geophys. Res. Atmos.,* 115, D221210.

Loader, N.J., Robertson, I., Switsur, V.R., Waterhouse, J.S. (1997), An improved technique for the batch processing of small whole wood samples to α-cellulose. *Chem. Geol.,* 136,

313-317.

Marchin, R., Broadhead, A.A., Bostic, L.E., Dunn, R.R., Hoffmann, W.A. (2016), Stomatal acclimation to vapour pressure deficit doubles transpiration of small tree seedlings with warming. *Plant Cell Environ.*, doi: 10.1111/pce.12790

McCarroll, D., Loader, N.J. (2004), Stable isotopes in tree rings. *Quat. Sci. Rev.,* 23, 771-801

McMahon, S.M., Parker, G.G., Miller, D.G. (2010), Evidence for a recent increase in forest growth. *Proc. Natl. Acad. Sci. USA,* 107, 3611-3615

Novick, K.A., Ficklin, D.L., Stoy, P.C., Williams, C.A., Bohrer, G., Oishi, A.C., Papuga, S.A., Blanken, P.D., Noormets, A., Sulman, B.N., Scott, R.L., Wang, L., Phillips, R.P. (2016), The increasing importance of atmospheric demand for ecosystem water and carbon fluxes. *Nature Clim. Change,* 6, 1023–1027, Doi: 10.1038/NCLIMATE3114

Rebetez, M., Saurer, M., Cherubini. P. (2003), To what extent can oxygen isotopes in tree rings and precipitation be used to reconstruct past atmospheric temperature? A case study. *Clim. Change*, 61, 237-248

Restaino, C.M., Peterson, D.L., Littell, J. (2016), Increased water deficit decreases Douglas fir growth throughout western US forests. *Proc. Natl. Acad. Sci. USA,* 113(34), 9557-9562

Roden, J.S., Lin, G., Ehleringer, J.R. (2000), A mechanistic model for interpretation of hydrogen and oxygen isotope ratios in tree-ring cellulose. *Geochim. Cosmochim. Acta*, 64, 21-35

Sarris, D., Siegwolf, R., Körner, C. (2013), Inter- and intra-annual stable carbon and oxygen isotope signals in response to drought in Mediterranean pines. *Agri. Forest Meteorol.* 168,

59-68

Saurer, M., Kirdyanov, A.V., Prokushkin, A.S., Rinne, K.T., Siegwolf, R. (2015), The impact of an inverse climate–isotope relationship in soil water on the oxygen-isotope composition of *Larix gmelinii* in Siberia. *New Phytol.,* 209, 955-964

Saurer., M., Kress, A., Leuenberger, M., Rinne, K.T., Treydte, K.S., Siegwolf, R. (2012), The influence of atmospheric circulation patterns on the oxygen isotope ratio of tree-rings in the Alpine region. *J. Geophys. Res. Atmos.*, 117, D05118.

Shi, C., Masson-Delmotte, V., Risi, C., Eglin, T., Stievenard, M., Pierre, M., Wang, X., Gao, J., Breon, F.M., Zhang, Q., Daux, V. (2011), Sampling strategy and climatic implications of tree-ring stable isotopes on the southeast Tibetan Plateau. *Earth Planet Sci. Lett.*, 301(1-2), 307-316. doi: 10.1016/j.epsl.2010.11.014

Shu, Y., Feng, X., Gazis, C., Anderson, D., Faiia, A.M., Tang, K., Ettl, J. (2005), Relative humidity recorded in tree rings: a study along a precipitation gradient in the Olympic Mountains, Washington, USA. *Geochim. Cosmochi. Acta,* 69(4), 791-799

Sidorova, O.V., Saurer, M., Bryukhanova, M.V., Siegwolf, R.T.W., Bigler, C. (2016), Site-specific water-use strategies of mountain pine and larch to cope with recent climate change. *Tree Physiol.,* 36: 942-953

Sidorova, O.V., Siegwolf, R.T.W., Saurer, M., Shashkin, A.V., Knorre. A.A., Prokushkin, A.S., Vaganov, E.A., Kirdyanov, A.V. (2009), Do centennial tree-ring and stable isotopes trends of *Larix gmelinii* (Rupr.) Rupr. indicate water storage in the Siberian north? *Clim. Dyn.*, 161, 825-835

Song, X., Clark, K.S., Helliker, B.R. (2014), Interpreting species-specific variation in tree

ring oxygen isotope ratios among three temperate forest trees. *Plant Cell Environ., 37(9),* 2169-2182

Sternberg, L.S.L.O. (2008), Oxygen stable isotope ratios of tree-ring cellulose: the next phase of understanding. *New Phytol.,* 181, 553-562

Sulman, B.N., Roman, D.T., Yi, K., Wang, L., Phillips, R.P., Novick, K.A. (2016), High atmospheric demand for water can limit forest carbon uptake and transpiration as severely as dry soil. *Geophys. Res. Lett.*, 43, 9686-9695. doi: 10.1002/2016GL069416

Szymczak, S., Joachimski, M., Bräuning, A., Hetzer, T., Kuhlemann, J. (2012), Are pooled tree ring $\delta^{13}C$ and $\delta^{18}O$ series reliable climate archives? A case study of *Pinus nigra* spp. [sic] *laricio* (Corsica/France), *Chem. Geol.,* 308–309: 40-49. doi: 10.1016/j.chemgeo.2012.03.013

Tang, K., Feng, X. (2001), The effect of soil hydrology on the oxygen and hydrogen isotopic compositions of plants' source water. *Earth Planet Sci. Lett.*, 185(3), 355-367.

Treydte, K., Boda, S., Pannatier, E.G., Fonti. P., Frank, D., Ullrich, B., Saurer, M., Siegwolf, R., Battipaglia, G., Werner, W., Gessler, A. (2014), Seasonal transfer of oxygen isotopes from precipitation and soil to the tree ring: source water versus needle water enrichment. *New Phytol.,* 202(3), 772-783.

Treydte, K.S., Schleser, G.H., Helle, G., Frank, D.C., Winiger, M., Haug, G., Esper, J. (2006), The twentieth century was the wettest period in northern Pakistan over the past millennium. *Nature,* 440, 1179-1182

Vicente-Serrano, S.M., Beguería, S., López-Moreno, J.I. (2010), A multiscalar drought index sensitive to global warming: the standardized precipitation evapotranspiration index. *J.*

Clim., 23(7): 1696-1718. doi: 10.1175/2009jcli2909.1

Wang, X.C., Song, L.P. (2011), Climate-tree growth relationships of *Pinus sylvestris* var. *mongolica* in the northern Daxing'an mountains, China. *Chinese J. Plant Ecol.,* 35(3), 294-302

Williams, A.P., Allen, C.D., Macalady, A.K., et al. (2013), Temperature as a potent driver of regional forest drought stress and tree mortality. *Nature Clim. Change,* 3, 292–297. doi: 10.1038/nclimate1693.

Xu, G., Liu, X., Wu, G., Chen, T., Wang, W., Zhang, Q., Zhang, Y., Zeng, X., Qin, D., Sun, W., Zhang, X. (2015), Tree ring δ^{18}O's indication of a shift to a wetter climate since the 1880s in the western Tianshan Mountains of northwestern China. *J. Geophys. Res. Atmo.,* 120, 6409–6425, doi: 10.1002/2014JD023027.

Zeng, X., Liu, X., Evans, M., Wang, W., An, W., Xu, G., Wu, G. (2016), Seasonal incursion of Indian Monsoon humidity and precipitation onto the southeastern Qinghai-Tibetan Plateau inferred from tree ring δ^{18}O values with intra-seasonal resolution. *Earth Planet Sci. Lett.,* 443, 9-19. doi: 10.1016/j.epsl.2016.03.011.

Zhang, X., Bai, X., Chang, Y., Chen, Z. (2016), Increased sensitivity of Dahurian larch radial growth to summer temperature with the rapid warming in Northeast China. *Trees,* 30, 1799-1806

Zhang, X., Liu, X., Zhang, Q., Wang, W., Zeng, X., Wu, G. (2017), Species-specific tree-growth response to climatic change in the northern Great Hinggan Mountains of permafrost region, northeastern China. *J. Glaciol. Geocryol.,* 38, in press. (in Chinese)
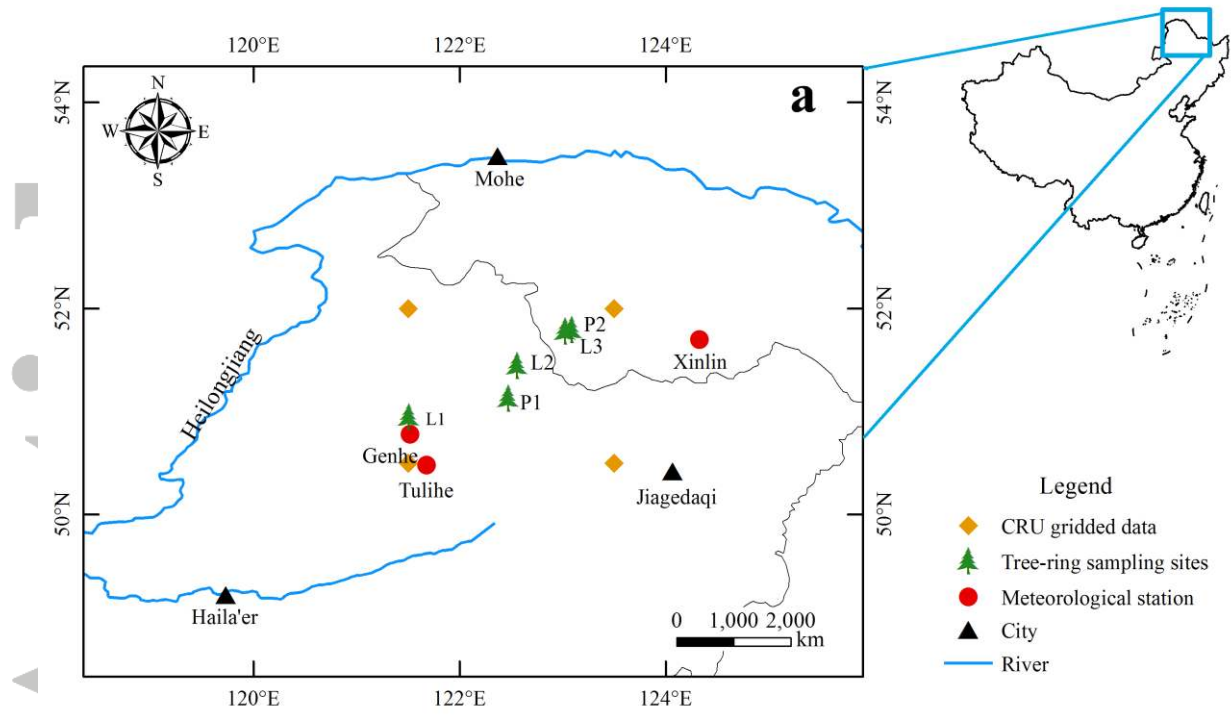
Zhang, Y., Liang, S. (2014), Changes in forest biomass and linkage to climate and forest

disturbances over Northeastern China. *Glob. Change Biol.,* 20(8), 2596-2606. doi: 10.1111/gcb.12588

Zhao, L., Xiao, H., Zhou, Ma., Cheng, G., Wang, L., Yin, L., Ren, J. (2012), Factors controlling spatial and seasonal distributions of precipitation $\delta^{18}O$ in China. *Hydrol. Process,* 26, 143-152
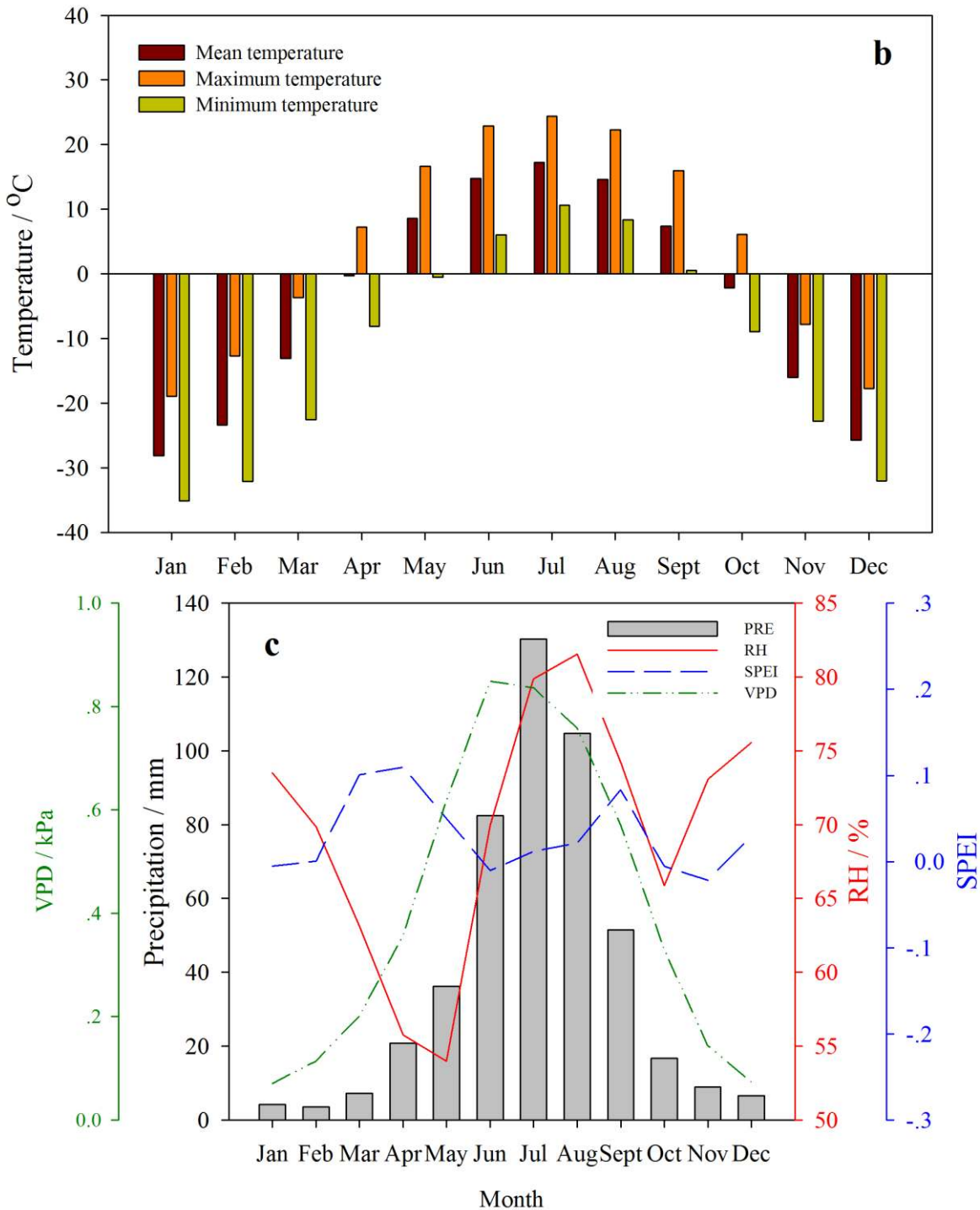
Figure 1 (a) Locations of sampling sites, nearby meteorological stations, and cells in the CRU grid used in this study. Sites L1 to L3 are for the larch trees; sites P1 and P2 are for the pine trees. (b) Monthly mean, maximum, and minimum temperatures and (c) monthly moisture conditions from 1957 to 2003. PRE, precipitation; RH, relative humidity; SPEI, standardized precipitation-evapotranspiration index; VPD, vapor-pressure deficit.
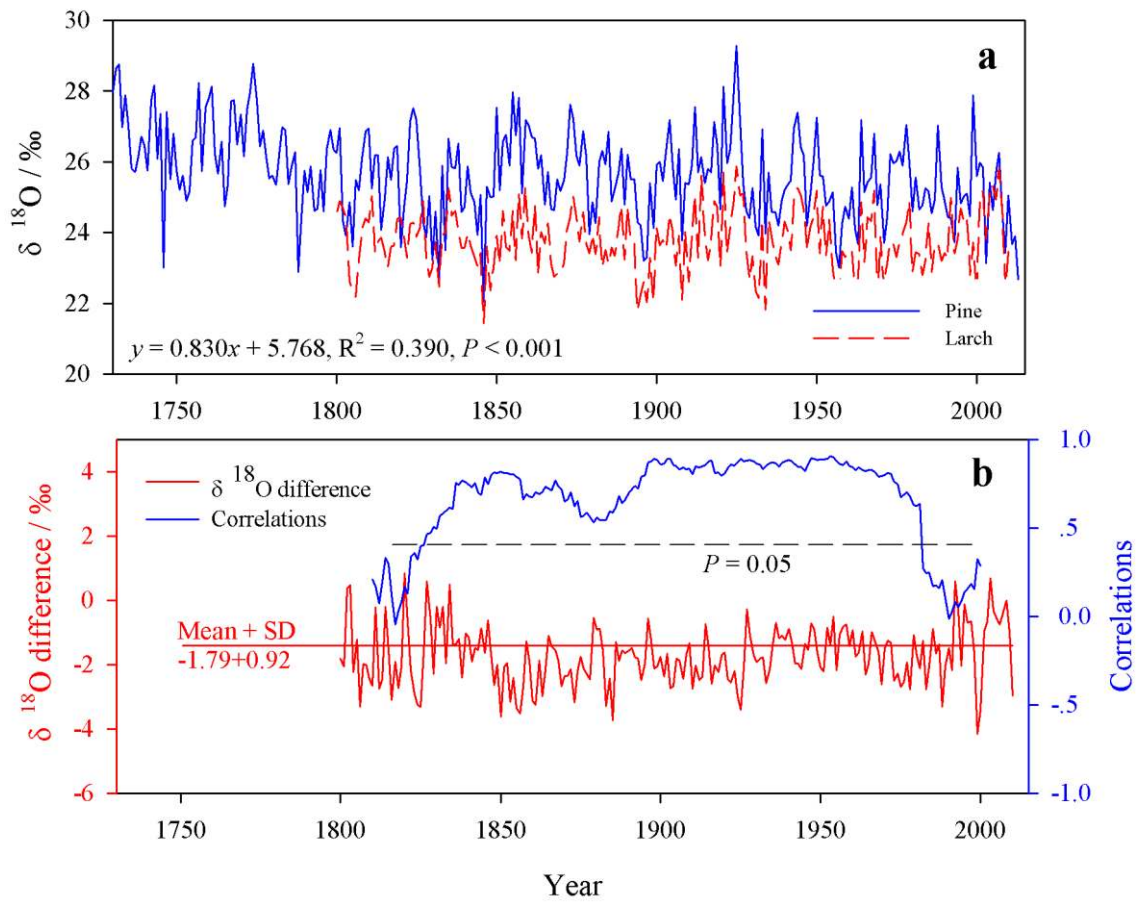
Figure 2 (a) Tree-ring $\delta^{18}O$ chronologies of larch and pine. (b) Difference in $\delta^{18}O$ of tree

rings (larch minus pine) and the 21-year sliding correlations between $\delta^{18}O$ values of the two

tree species.

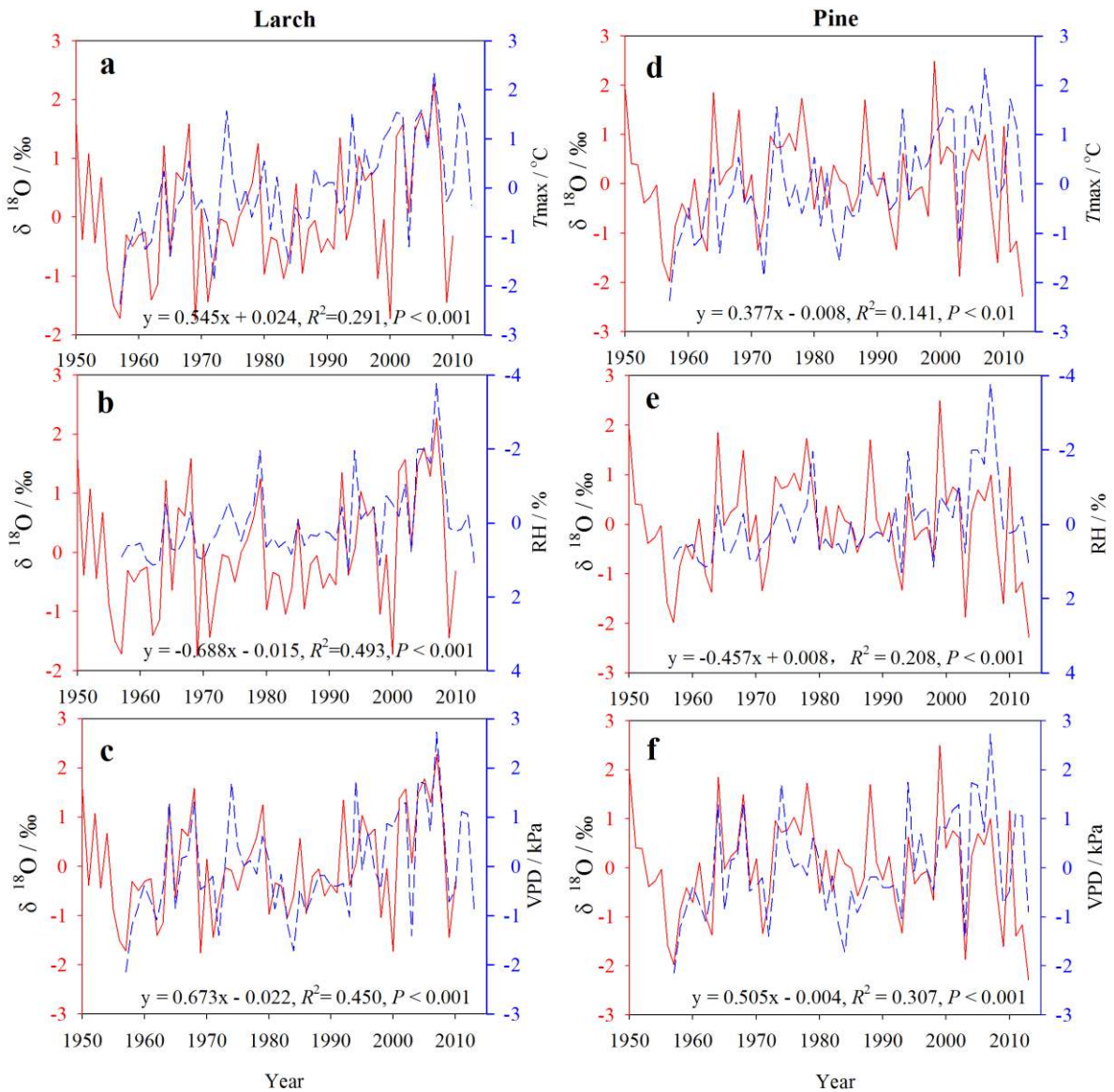**Figure 3** Comparisons of temporal trends between tree-ring $\delta^{18}O$ and significant climatic parameters from July to August for yearly (YE) variations. The left column is for larch and the right column is for pine. The climatic parameters include (a, d) the monthly mean maximum temperature (T_{max}), (b, e) relative humidity (RH), and (c, f) vapor-pressure deficit (VPD) from July to August. All data were normalized as Z-scores.
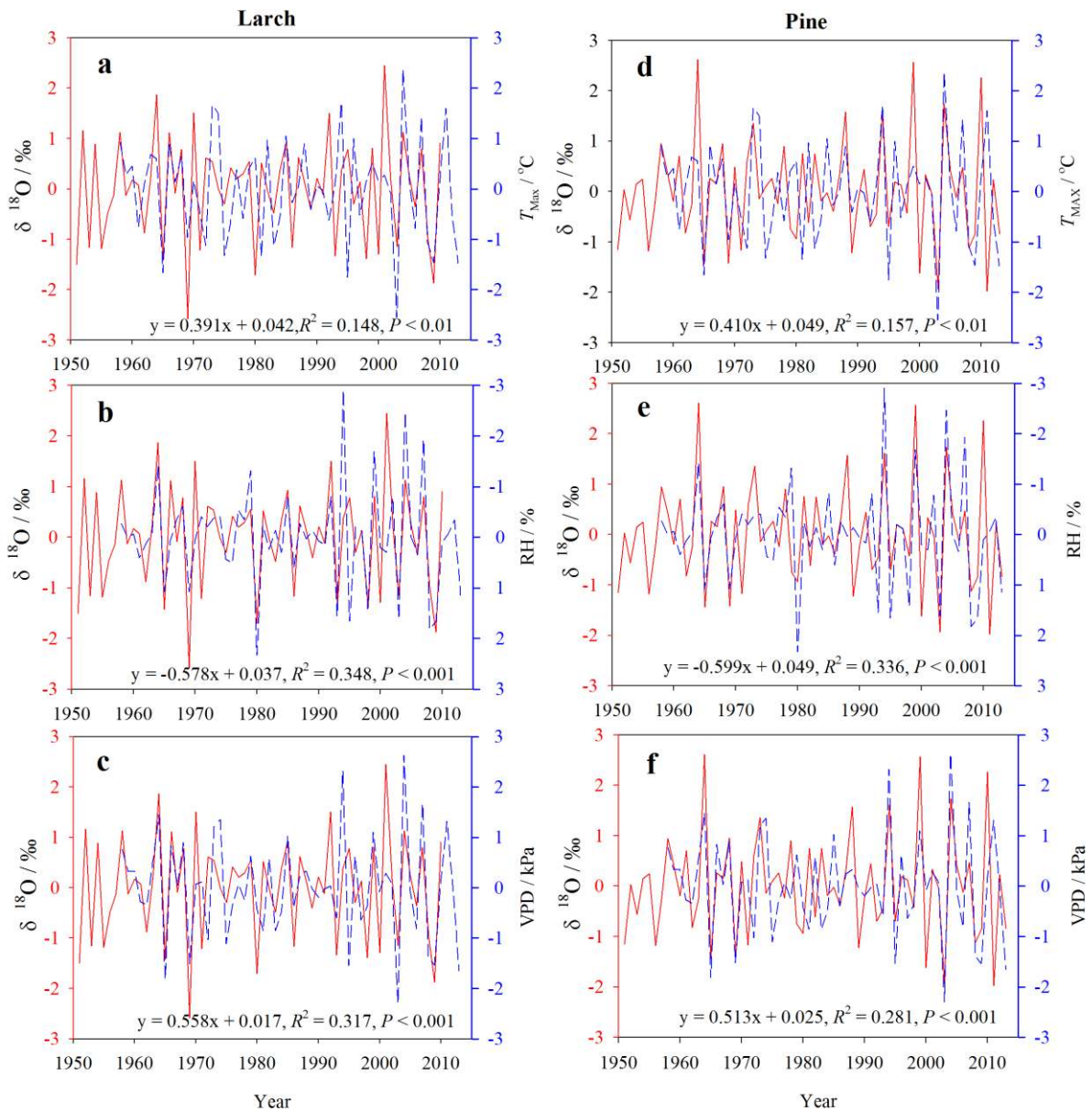
Figure 4 Comparisons of temporal trends between tree-ring δ^{18}O and significant climatic parameters from July to August for variation in the first-order difference (FOD). The left column is for larch and the right column is for pine. The climatic parameters include (a, d) the monthly mean maximum temperature (T_{max}), (b, e) relative humidity (RH), and (c, f) vapor-pressure deficit (VPD) from July to August. All data were normalized as Z-scores.
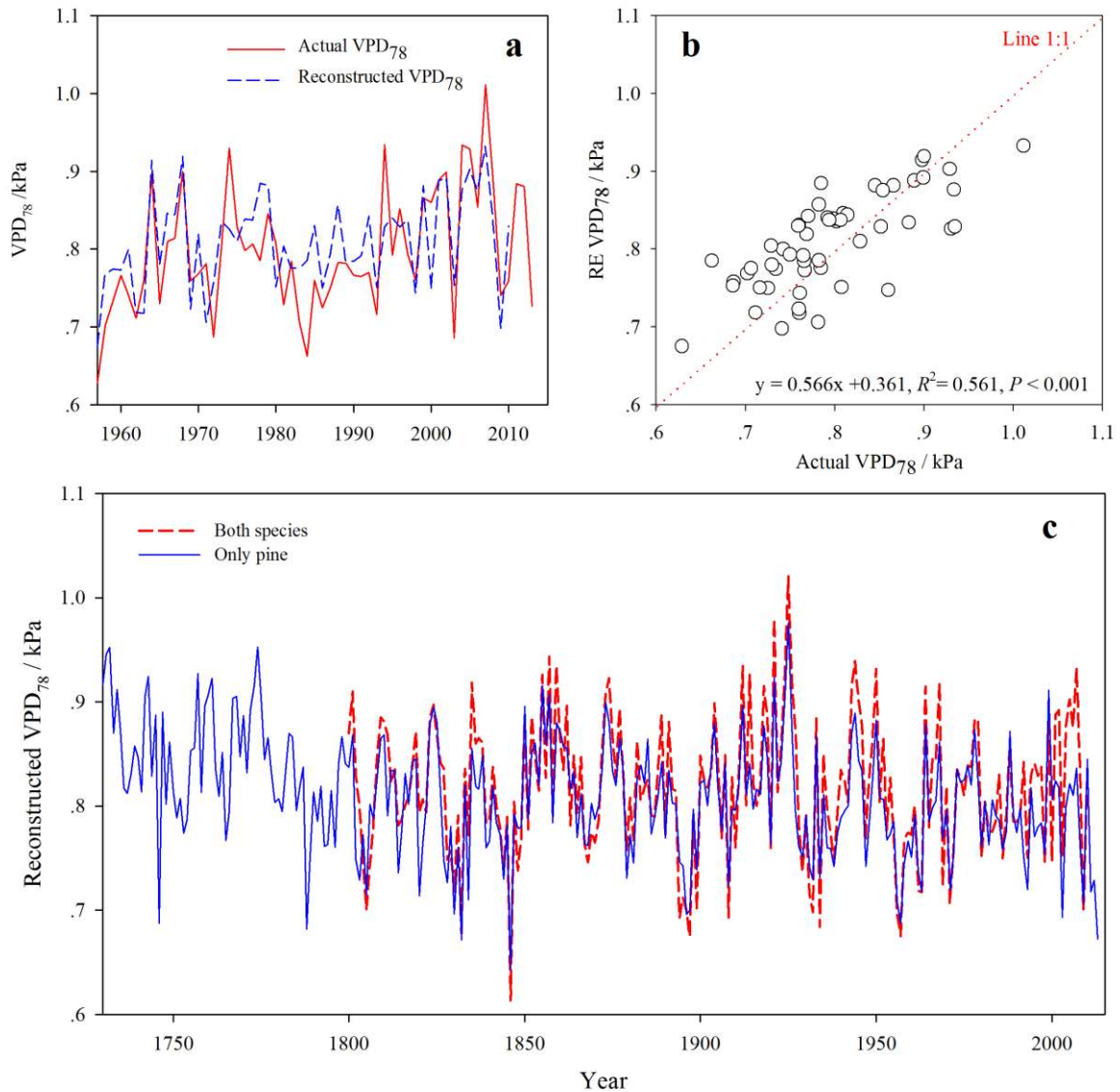
Figure 5 (a) Reconstruction of the July to August vapor-pressure deficit (VPD_{78}). (a) Comparison of actual and reconstructed VPD from July to August. (b) Scatterplot of actual and reconstructed VPD from July to August. In pane b, an outlier from 1971 was removed. The regression functions and proportion of the variance explained are provided. (c) Comparison of the reconstructed VPD from July to August based on both $\delta^{18}O$ chronologies (from larch and pine), and based only on the $\delta^{18}O$ chronology from pine.
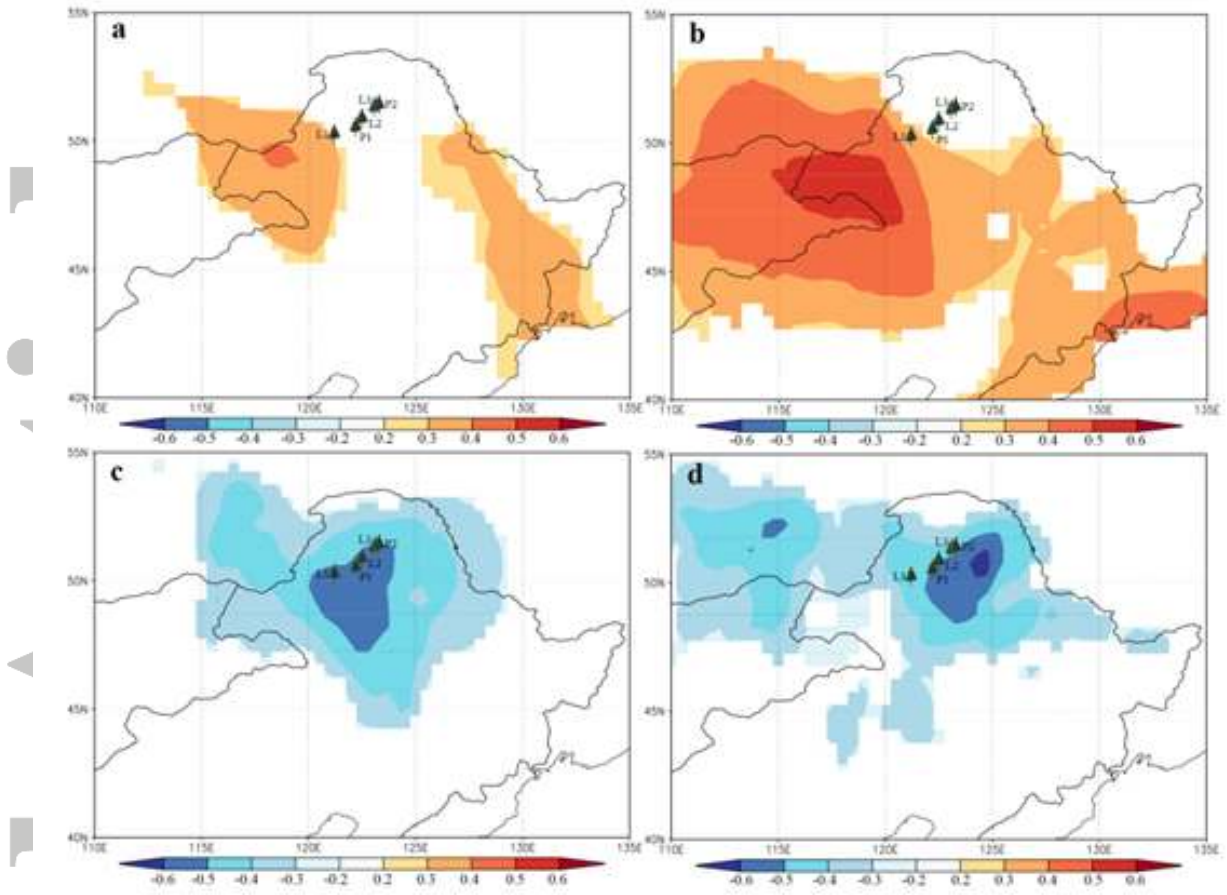
Figure 6 Spatial correlations between the reconstructed VPD from July to August and the mean (a, b) CRU temperature and (c, d) precipitation time series for the four nearest cells in the CRU grid (Figure 1a). The period for panes (a) and (c) is from 1901 to 1956; the period for panes (b) and (d) is from 1957 to 2010. Only the statistically significant correlations (*P* <0.01) were shown.
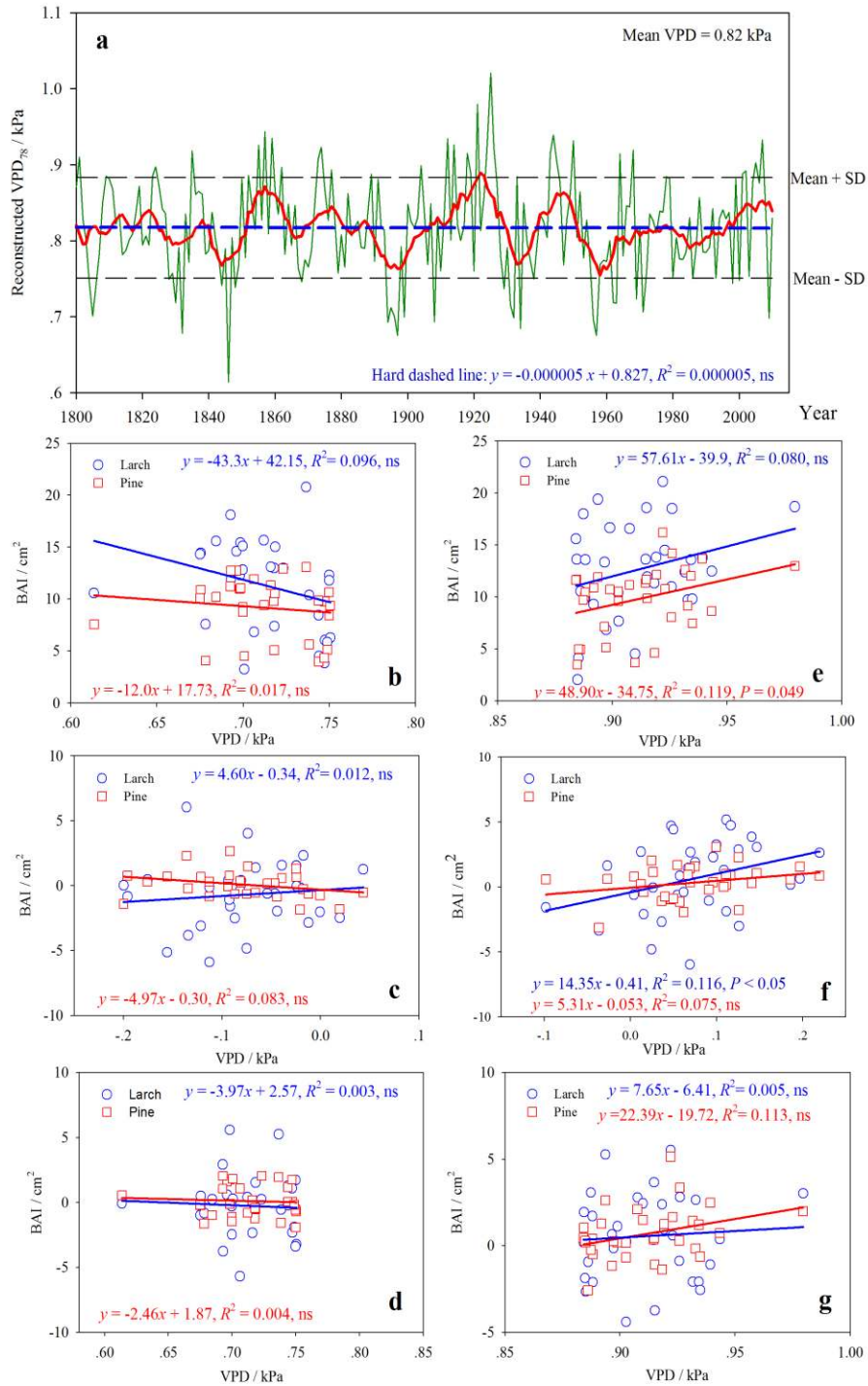
Figure 7 (a) Changes in the reconstructed vapor-pressure deficit (VPD) since 1800. The solid red line is the smoothed curve with an 11-year moving window analysis for the reconstructed VPD_{78}. The horizontal dashed blue line is the linear fit for the reconstructed VPD_{78}; the regression for this line was not significant. (b, c, d) Scatterplots for the relationship between

the basal area increment (BAI) and VPD for years with values less than the mean − 1SD. (e, f, g) Scatterplots for the relationship between BAI and VPD for years with values greater than the mean + 1SD. (b, e) yearly variations, (c, f) first-order difference variations, (d, g) BAI variations with the low-frequency variations removed (Fig. S4c).

Table 1 Calibration and verification statistics for the reconstructed July to August vapor-pressure deficit (VPD). *r*, Pearson's correlation coefficient; R^2, regression goodness of fit; ST, sign test (±); RE, reduction of error; CE, coefficient of efficiency.

	Calibration	*r*	R^2	R^2_{adj}	ST	Verification	RE	CE	ST
Split/cross calibration	1957-1984	0.735	0.540	0.527	24+/3-	1985-2010	0.472	0.526	19+/7-
	1985-2010	0.753	0.568	0.549	19+/7-	1957-1984	0.447	0.509	24+/3-
Leave-one-out	1957-2010	0.684	0.468	0.457	39+/14-				